

Research Article

Numerical Study of a Thermally Stressed State of a Rod

Anarbay Kudaykulov,¹ Erkin Arinov,² Nurlybek Ispulov ,³
Abdul Qadir ,⁴ and Kalamkas Begaliyeva⁵

¹Institute of Information and Computational Technologies CS MES RK, Almaty, Kazakhstan

²Zhezkazgan University named after O.A. Baykonurov, Zhezkazgan, Kazakhstan

³S. Toraighyrov Pavlodar State University, Pavlodar, Kazakhstan

⁴Department of Electrical Engineering, Sukkur IBA University, Sindh, Pakistan

⁵Al-Farabi Kazakh National University, Almaty, Kazakhstan

Correspondence should be addressed to Abdul Qadir; aqadir@iba-suk.edu.pk

Received 26 February 2019; Accepted 21 April 2019; Published 2 June 2019

Academic Editor: Zine El Abiddine Fellah

Copyright © 2019 Anarbay Kudaykulov et al. This is an open access article distributed under the Creative Commons Attribution License, which permits unrestricted use, distribution, and reproduction in any medium, provided the original work is properly cited.

This paper considers a new method based on the law of energy conservation for the study of thermo-stress-strain state of a rod of limited length with simultaneous presence of local heat fluxes, heat exchanges, and thermal insulation. The method allows determining the field of temperature distribution and the three components of deformations and stresses, as well as the magnitude of the rod elongation and the resulting axial force with an accuracy of satisfying the energy conservation laws. For specific initial data, all the sought-for ones are determined numerically with high accuracy. We found that all solutions satisfy the laws of energy conservation.

1. Introduction

This work is devoted to the study of the thermo-stress-strain state of a rod of constant cross section and of limited length. In this case, a heat flux of constant intensity is supplied to a closed local surface. The rest of the side surface of the rod is fully thermally insulated. Through the cross-sectional area of the two ends of the rod, convective heat exchange with the environment occurs. In this case, the coefficients of heat transfer and the temperature of the surrounding medium at the two ends of the rod are different. To determine the temperature field, the energy conservation law is used in the form of the total heat energy functional taking into account the existing dissimilar types of heat sources, physical and mechanical properties of the rod material, and its geometrical dimensions. Using this, the law of temperature distribution along the length of the rod under study is constructed. They determine the magnitude of the elongation of the rod, in the case of pinching one end. If both ends of the rod are clamped, then the magnitude of the resulting axial force is determined. The laws of distribution of thermoelastic, temperature, and

elastic components of deformations and stresses are also determined depending on the presence of local heat flux, thermal insulation of heat exchanges, the geometry of the rod, and the physic-mechanical properties of the material of the rod. To determine the displacement field, the energy conservation law is used in the form of the potential energy functional of elastic deformation taking into account the presence of a temperature field. Further, the displacement field is determined taking into account the actual operating conditions. The developed program allows varying the values of the source data.

In [1], the fundamental laws of the theory of thermoelasticity for deformable solids are given. In [2, 3], the results of a numerical study of a thermo-stress-deformed state of a rod under the action of laser beams are presented. In this case, the finite element method was used. The application of the finite element method is given in [4]. In [5], the exact solution of a two-dimensional definition problem in an ideally elastic-plastic cylindrical rod with a given uniform internal temperature is given. The dependence of voltage on temperature in a rod of limited length is given in [6]. In

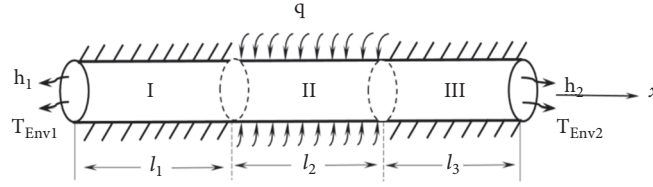


FIGURE 1: The design scheme of the problem.

this work, the temporary factor is also taken into account. In [7], different statements of problems of thermal elasticity are given for structural elements under temperature effects. In this case, the theoretical basis of the method is focused on the Maysel formula of uncoupled thermoelasticity. In [8], on the basis of the small parameter method, the problem of determining the stress-strain state of an elastic-plastic pipe in the presence of temperature is considered. It uses the terms of Mises. In [9], the fundamentals of the theory of thermoelasticity and methods for their implementation in solving specific applied problems are presented. This takes into account the power and temperature factors. In the works [10, 11] methods and computational algorithms for numerical solution of the class of applied problems of mechanics are presented.

In contrast to the above works, this paper uses the fundamental energy conservation laws in combination with the constructed quadratic spline functions to solve a particular applied problem.

2. Formulation of the Problem and Methods

We consider a horizontal bar of limited length L [cm], and a constant cross section F [cm²]. The horizontal axis ox we will direct from the left to right coincides with the axis of the rod. The side surfaces of the sections ($0 \leq x \leq l_1$) and ($l_2 \leq x \leq L$) the core are fully thermally insulated. A heat flux of constant intensity q [W/cm²] is supplied on the lateral surface of the rod section ($l_1 \leq x \leq l_2$). Through the cross-sectional area of the left and right ends of the rod, heat exchange with the environment takes place.

Heat transfer coefficients at $x = 0$ and at $x = L$ [W/cm²]. The temperature of the environments of these areas are T_{Env1} and T_{Env2} [°K], respectively. The design scheme of the problem is shown in Figure 1.

3. The Solution to the Problem Using the Energy Conservation Law

The rod under consideration is discretized by elements of length L [cm]. Within the length of one discrete element, we approximate the temperature field by a second-order polynomial

$$T(x) = ax^2 + bx + c, \quad 0 \leq x \leq l \quad (1)$$

where a , b , c are constants, the values of which are still unknown. The law of temperature distribution within the length of one discrete element is shown in Figure 2.

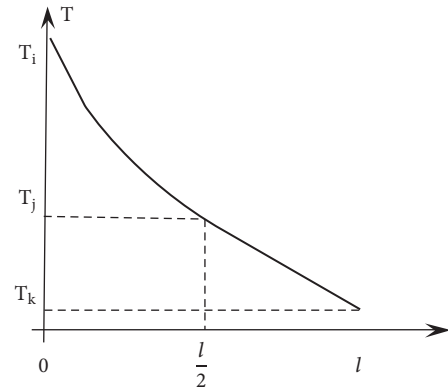


FIGURE 2: The law of temperature distribution along the length of one discrete element.

In the local coordinate system $0 \leq x \leq l$, we fix three nodes with coordinates $x_i = 0$; $x_j = l/2$; $x_k = l$.

The temperature values in these sections will be denoted, respectively, by the following.

$$\begin{aligned} T(x = x_i = 0) &= T_i; \\ T\left(x = x_j = \frac{l}{2}\right) &= T_j; \\ T(x = x_k = l) &= T_k \end{aligned} \quad (2)$$

Then substituting (2) into (1), we get the following system.

$$\begin{aligned} a \cdot 0 + b \cdot 0 + c &= T_i \\ a \cdot \left(\frac{l}{2}\right)^2 + b \cdot \left(\frac{l}{2}\right) + c &= T_j \\ a \cdot l^2 + b \cdot l + c &= T_k \end{aligned} \quad (3)$$

Solving the system, we define the following.

$$\begin{aligned} c &= T_i; \\ b &= \frac{4T_j - 3T_i - T_k}{l}; \\ a &= \frac{2T_k + 2T_i - 4T_j}{l^2} \end{aligned} \quad (4)$$

Substituting (4) into (1), we have the following.

$$\begin{aligned} T(x) &= \frac{2T_k + 2T_i - 4T_j}{l^2} \cdot x^2 + \frac{4T_j - 3T_i - T_k}{l} \cdot x + T_i \\ &= \left(\frac{2x^2 - 3lx + l^2}{l^2} \right) T_i + \left(\frac{4lx - 4x^2}{l^2} \right) T_j \\ &\quad + \left(\frac{2x^2 - lx}{l^2} \right) T_k, \quad 0 \leq x \leq l \end{aligned} \quad (5)$$

Here we introduce the following notations.

$$\begin{aligned} \varphi_i(x) &= \frac{2x^2 - 3lx + l^2}{l^2}; \\ \varphi_j(x) &= \frac{4lx - 4x^2}{l^2}; \\ \varphi_k(x) &= \frac{2x^2 - lx}{l^2}, \end{aligned} \quad (6)$$

$$0 \leq x \leq l$$

These functions are called quadratic spline functions in the local coordinate system. They have the following properties.

$$\begin{aligned} \varphi_i(x) &= \begin{cases} 1, & \text{at } x = 0 \\ 0, & \text{at } x = \frac{l}{2} \\ 0, & \text{at } x = l; \end{cases} \\ \varphi_j(x) &= \begin{cases} 0, & \text{at } x = 0 \\ 1, & \text{at } x = \frac{l}{2} \\ 0, & \text{at } x = l; \end{cases} \\ \varphi_k(x) &= \begin{cases} 0, & \text{at } x = 0 \\ 0, & \text{at } x = \frac{l}{2} \\ 1, & \text{at } x = l; \end{cases} \end{aligned} \quad (7)$$

$$\varphi_i(x) + \varphi_j(x) + \varphi_k(x) = 1; \quad 0 \leq x \leq l \quad (8)$$

The temperature gradient within the length of one discrete element in the local coordinate system has the following form.

$$\begin{aligned} \frac{\partial T}{\partial x} &= \frac{\partial \varphi_i(x)}{\partial x} T_i + \frac{\partial \varphi_j(x)}{\partial x} T_j + \frac{\partial \varphi_k(x)}{\partial x} T_k \\ &= \frac{4x - 3l}{l^2} T_i + \frac{4l - 8x}{l^2} T_j + \frac{4x - l}{l^2} T_k, \quad 0 \leq x \leq l \end{aligned} \quad (9)$$

Here the following should be noted.

$$\frac{\partial \varphi_i(x)}{\partial x} T_i + \frac{\partial \varphi_j(x)}{\partial x} T_j + \frac{\partial \varphi_k(x)}{\partial x} T_k = 0 \quad (10)$$

To construct resolving systems of equations taking into account the natural boundary conditions, we discretize the rod under study by three elemental lengths. For the first discrete element, the total energy functional with the thermal insulation of the side surface is as follows.

$$J_1 = \int_{S(x=0)} \frac{h_1}{2} (T - T_{oc1})^2 ds + \int_{V_1} \frac{K_{xx}}{2} \left(\frac{\partial T}{\partial x} \right)^2 dv, \quad (11)$$

$$(0 \leq x \leq l_1)$$

Here the first integral over the cross-sectional area of the left end takes place only for points of this surface. In the local coordinate system, taking into account the global node indexing, (11) can be rewritten in the following form:

$$\begin{aligned} J_1 &= \frac{F(x=0) h_1}{2} (T - T_{oc1})^2 + \frac{FK_{xx}}{2} \\ &\cdot \int_0^l \left[\left(\frac{4x - 3l_1}{l_1^2} T_1 + \frac{4l_1 - 8x}{l_1^2} T_2 \right. \right. \\ &\quad \left. \left. + \frac{4x - l_1}{l_1^2} T_3 \right) \right]^2 dx = \frac{Fh_1}{2} (T_1 - T_{oc1})^2 \\ &\quad + \frac{FK_{xx}}{6l_1} [7T_1^2 - 16T_1T_2 + 2T_1T_3 - 16T_2T_3 + 16T_2^2 \\ &\quad + 7T_3^2] \end{aligned} \quad (12)$$

where h_1 is the heat transfer coefficient.

Here it must be said that the lateral surface of the first discrete element is fully thermally insulated. In expression (12), it should be noted that the sum of the coefficients before the nodal values of temperature will be zero. For example, in the first bracket $(1-1) = 0$, and in the second bracket $[7-16 + 2-16 + 16 + 7] = 0$. Now in Figure 1 we consider the second discrete element. This item is internal. But on the side surface of this element summed thermal constant intensity $q[W/cm^2]$, the total heat energy functional will have the following form.

$$\begin{aligned} J_2 &= \int_{V_2} \frac{K_{xx}}{2} \left(\frac{\partial T}{\partial x} \right)^2 dv + \int_{S_{\text{side}}} qT ds = \frac{FK_{xx}}{2} \\ &\cdot \int_0^l \left[\left(\frac{4x - 3l_2}{l_2^2} T_3 + \frac{4l_2 - 8x}{l_2^2} T_4 \right. \right. \\ &\quad \left. \left. + \frac{4x - l_2}{l_2^2} T_5 \right) \right]^2 dx \\ &\quad + qP \int_0^l \left[\left(\frac{2x^2 - 3l_2x + l_2^2}{l_2^2} \right) T_3 \right. \end{aligned}$$

$$\begin{aligned}
& + \left(\frac{4l_2x - 4x^2}{l_2^2} \right) T_4 + \left(\frac{2x^2 - l_2x}{l_2^2} \right) T_5 \Big] dx \\
& = \frac{FK_{xx}}{6l_2} [7T_3^2 - 16T_3T_4 + 2T_3T_5 - 16T_4T_5 + 16T_4^2 \\
& + 7T_5^2] + \frac{q\pi r l_2}{3} (T_3 + 4T_4 + T_5), \quad (l_1 \leq x \leq l_2)
\end{aligned} \tag{13}$$

Here V_2 is the volume of the second discrete element; $P = 2\pi k$ is the perimeter of the cross section. Finally go to the last third discrete element. The side surface of this element is fully insulated, but through the cross-sectional area of the right end there is a heat exchange with its environment. In this case, the heat transfer coefficient is h_2 , and the ambient temperature is T_{Env2} . The length of this item is l_3 . The total heat energy functional for the third discrete element will be as follows:

$$\begin{aligned}
J_3 = & \int_{V_3} \frac{K_{xx}}{2} \left(\frac{\partial T}{\partial x} \right)^2 dv + \int_{S(x=l_1+l_2+l_3)} \frac{h_2}{2} (T \\
& - T_{oc2})^2 ds = \frac{FK_{xx}}{2} \int_0^l \left[\left(\frac{4x - 3l_3}{l_3^2} \right) T_5 \right. \\
& \left. + \left(\frac{4l_3 - 8x}{l_3^2} \right) T_6 + \left(\frac{4x - l_3}{l_3^2} \right) T_7 \right]^2 dx
\end{aligned}$$

$$\begin{aligned}
& + \frac{Fh_2}{2} (T_7 - T_{oc2})^2 = \frac{FK_{xx}}{6l_3} [7T_5^2 - 16T_5T_6 \\
& + 2T_5T_7 - 16T_6T_7 + 16T_6^2 + 7T_7^2] + \frac{Fh_2}{2} (T_7 \\
& - T_{oc2})^2, \quad (l_2 \leq x \leq L)
\end{aligned} \tag{14}$$

where V_3 is the volume of the third discrete element and F is the cross-sectional area of the rod; then the total heat energy functional for the rod under study has the following form.

$$\begin{aligned}
J = J_1 + J_2 + J_3 = & \frac{Fh_1}{2} (T_1 - T_{oc1})^2 + \frac{FK_{xx}}{6l_1} \times [7T_1^2 \\
& - 16T_1T_2 + 2T_1T_3 - 16T_2T_3 + 16T_2^2 + 7T_3^2] \\
& + \frac{FK_{xx}}{6l_2} \times \frac{FK_{xx}}{6l_2} \cdot [7T_3^2 - 16T_3T_4 + 2T_3T_5 \\
& - 16T_4T_5 + 16T_4^2 + 7T_5^2] + \frac{q\pi r l_2}{3} (T_3 + 4T_4 + T_5) \\
& + \frac{FK_{xx}}{6l_3} [7T_5^2 - 16T_5T_6 + 2T_5T_7 - 16T_6T_7 + 16T_6^2 \\
& + 7T_7^2] + \frac{Fh_2}{2} (T_7 - T_{oc2})^2
\end{aligned} \tag{15}$$

To construct resolving systems of linear algebraic equations for the nodal values of temperatures, the functional J is minimized by T_1, T_2, \dots, T_7 .

$$(1) \quad \frac{\partial J}{\partial T_1} = 0;$$

$$\Rightarrow Fh_1 (T_1 - T_{Env1}) + \frac{FK_{xx}}{6l_1} [14T_1 - 16T_2 + 2T_3]$$

$$= 0;$$

$$(2) \quad \frac{\partial J}{\partial T_2} = 0;$$

$$\Rightarrow \frac{FK_{xx}}{6l_1} [-16T_1 + 32T_2 - 16T_3] = 0;$$

$$(3) \quad \frac{\partial J}{\partial T_3} = 0;$$

$$\Rightarrow FK_{xx} \left[\left(\frac{2T_1 + 16T_2 + 14T_3}{6l_1} \right) + \left(\frac{14T_3 - 16T_4 + 2T_5}{6l_2} \right) \right] + \frac{q\pi r l_2}{3} = 0;$$

$$(4) \quad \frac{\partial J}{\partial T_4} = 0;$$

$$\Rightarrow \frac{FK_{xx}}{6l_2} [-16T_3 + 32T_4 - 16T_5] + \frac{4q\pi r l_2}{3} = 0;$$

$$(5) \quad \frac{\partial J}{\partial T_5} = 0;$$

$$\Rightarrow FK_{xx} \left[\left(\frac{2T_3 - 16T_4 + 14T_5}{6l_2} \right) + \left(\frac{14T_5 - 16T_6 + 2T_7}{6l_3} \right) \right] + \frac{qprl_2}{3} = 0;$$

$$(6) \quad \frac{\partial J}{\partial T_6} = 0;$$

$$\Rightarrow \frac{FK_{xx}}{6l_3} [-16T_5 + 32T_6 - 16T_7] = 0;$$

$$(7) \quad \frac{\partial J}{\partial T_7} = 0;$$

$$\Rightarrow \frac{FK_{xx}}{6l_3} [2T_5 - 16T_6 + 14T_7] + Fh_2(T_7 - T_{Env2}) = 0.$$

(16)

Solving this system, the node values of temperatures T_1, T_2, \dots, T_7 are calculated. They are used to construct the law of temperature distribution along the length of three discrete sections of the rod.

$$\begin{aligned} T^{(I)}(x) &= \left(\frac{2x^2 - 3l_1x + l_1^2}{l_1^2} \right) T_1 + \left(\frac{4l_1x - 4x^2}{l_1^2} \right) T_2 \\ &\quad + \left(\frac{2x^2 - l_1x}{l_1^2} \right) T_3, \quad 0 \leq x \leq l_1 \\ T^{(II)}(x) &= \left(\frac{2x^2 - 3l_2x + l_2^2}{l_2^2} \right) T_3 + \left(\frac{4l_2x - 4x^2}{l_2^2} \right) T_4 \\ &\quad + \left(\frac{2x^2 - l_2x}{l_2^2} \right) T_5, \quad 0 \leq x \leq l_2 \\ T^{(III)}(x) &= \left(\frac{2x^2 - 3l_3x + l_3^2}{l_3^2} \right) T_5 + \left(\frac{4l_3x - 4x^2}{l_3^2} \right) T_6 \\ &\quad + \left(\frac{2x^2 - l_3x}{l_3^2} \right) T_7, \quad 0 \leq x \leq l_3 \end{aligned} \quad (17)$$

If the coefficient of thermal expansion of the material of the rod $\alpha [1/^\circ K]$ is a constant value, then the value of thermal elongation of the rod $\Delta l_T [cm]$ in case of pinching with one end is determined in accordance with the theory of thermal physics [11].

$$\Delta l_T = \int_0^L \alpha \cdot T(x) dx. \quad (18)$$

$$\text{where } T(x) = T^{(I)}(x) + T^{(II)}(x) + T^{(III)}(x) \quad (19)$$

If both ends of the rod are clamped, then it cannot lengthen, but there is an axial compressive force R [kG], which is determined by the conditions of compatibility deformation.

Then substituting (19) in (18), we get the following.

$$\begin{aligned} \Delta l_T &= \alpha \left[\frac{l_1}{6} T_1 + \frac{2l_1}{3} T_2 + \frac{l_1}{6} T_3 + \frac{l_2}{6} T_3 + \frac{2l_2}{3} T_4 + \frac{l_2}{6} T_5 \right. \\ &\quad \left. + \frac{l_3}{6} T_5 + \frac{2l_3}{3} T_6 + \frac{l_3}{6} T_7 \right] = \frac{\alpha}{6} [l_1 T_1 + 4l_1 T_2 \\ &\quad + (l_1 + l_2) T_3 + 4l_2 T_4 + (l_2 + l_3) T_5 + 4l_3 T_6 + l_3 T_7] \end{aligned} \quad (20)$$

If both ends of the rod are clamped, then it cannot lengthen, but there is an axial compressive force R [kG], which is determined by the conditions of compatibility deformation. The essence of this approach is as follows. First, consider the horizontal rod clamped by the left end (Figure 3).

This rod is under the influence of the compressive force R which is applied at the right free end. Then, according to Hooke's law, it is reduced by the value of Δl_R

$$\Delta l_R = \frac{R \cdot L}{E \cdot F} \quad (21)$$

where $L = l_1 + l_2 + l_3$ is the total length of the test rod, $E [kG/cm]$ modulus of elasticity of the material of the rod, and $F [cm^2]$ rod area.

If both ends of the rod under study are rigidly clamped, then naturally it does not lengthen or shorten; i.e.,

$$\Delta l_R + \Delta l_T = 0. \quad (22)$$

Then, taking into account (21), we will determine the value of the axial compressive force R that arises in the clamped rod by the two ends of the rod under study.

$$\begin{aligned} R &= -\frac{E \cdot F \cdot \Delta l_T}{L} = -\frac{E \cdot F \cdot \alpha}{6L} [l_1 T_1 + 4l_1 T_2 \\ &\quad + (l_1 + l_2) T_3 + 4l_2 T_4 + (l_2 + l_3) T_5 + 4l_3 T_6 + l_3 T_7] \end{aligned} \quad (23)$$

In this case, the distribution field of the thermoelastic component of stress $\sigma [kG/cm^2]$ also arises, which is determined in accordance with Hooke's law [1].

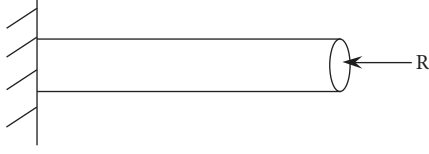


FIGURE 3: The left end of the rod is pinned under the influence of compressive force R [kG].

In this case, the distribution field of the thermoelastic component of stress σ [kG/cm²], which is determined in accordance with Hooke's law [1], also appears.

$$\sigma(x) = \frac{R}{F} = \text{const} \quad (24)$$

Then, according to Hooke's law, the field distribution of the thermoelastic component of deformation has the following form.

$$\varepsilon(x) = \frac{\sigma(x)}{E} = \text{const} \quad (25)$$

The field distribution of the temperature component of the strain and stress is determined on the basis of the general theory of thermoelasticity.

$$\varepsilon_T(x) = -\alpha T(x), \quad (26)$$

$$\sigma_T(x) = E \cdot \varepsilon_T(x) = -\alpha E T(x), \quad (27)$$

From these relations, in accordance with the theory of thermoelasticity, the field distribution of elastic components of deformations and stresses is determined.

$$\varepsilon_x(x) = \varepsilon - \varepsilon_T = \frac{\sigma(x)}{E} + \alpha \cdot T(x), \quad (28)$$

$$\sigma_x(x) = E \cdot \varepsilon_x(x) = \sigma(x) - \sigma_T(x), \quad (29)$$

The displacement field along the length of one discrete element of length l [cm] is approximated by a complete second-order polynomial.

$$U(x) = \varphi_i(x)U_i + \varphi_j(x)U_j + \varphi_k(x)U_k, \quad 0 \leq x \leq l \quad (30)$$

The gradient of displacement is determined from here

$$\frac{\partial u}{\partial x} = \frac{4x-3l}{l^2}U_i + \frac{4l-8x}{l^2}U_j + \frac{4x-l}{l^2}U_k, \quad 0 \leq x \leq l \quad (31)$$

where $U_i = U(x=0)$; $U_j = U(x=l/2)$; $U_k = U(x=l)$. The potential energy functional of elastic deformation in the presence of a temperature field has the following form [1].

$$\Pi = \int_V \frac{\sigma_x(x)}{2} \varepsilon_x(x) dv - \int_V \alpha E \cdot T(x) \cdot \varepsilon_x(x) dv \quad (32)$$

where $\varepsilon_x(x) = \partial U / \partial x = ((4x-3l)/l^2)U_i + ((4l-8x)/l^2)U_j + ((4x-l)/l^2)U_k$ is the elastic component of deformation; $\sigma_x(x) = E\varepsilon_x(x) = E(\partial U / \partial x) = E(((4x-3l)/l^2)U_i + ((4l-8x)/l^2)U_j + ((4x-l)/l^2)U_k)$ is the elastic component of stress.

Given these relations, the expression of the potential energy of other strains for the rod under study can be rewritten as follows.

$$\begin{aligned} \Pi = & \int_{V_1} \frac{\sigma_x(x)}{2} \varepsilon_x(x) dv - \int_{V_1} \alpha \cdot E \cdot T(x) \cdot \varepsilon_x(x) dv \\ & + \int_{V_2} \frac{\sigma_x(x)}{2} \varepsilon_x(x) dv - \int_{V_2} \alpha \cdot E \cdot T(x) \\ & \cdot \varepsilon_x(x) dv + \int_{V_3} \frac{\sigma_x(x)}{2} \varepsilon_x(x) dv - \int_{V_3} \alpha \cdot E \\ & \cdot T(x) \cdot \varepsilon_x(x) dv = \frac{EF}{2} \int_0^l \left[\frac{4x-3l}{l^2} U_1 \right. \\ & + \frac{4l-8x}{l^2} U_2 + \left. \frac{4x-l}{l^2} U_3 \right]^2 dx \\ & - \alpha EF \int_0^l \left[\frac{2x^2-3lx+l}{l^2} T_1 + \frac{4l-4x^2}{l^2} T_2 \right. \\ & + \left. \frac{2x^2-lx}{l^2} T_3 \right] \times \left[\frac{4x-3l}{l^2} U_1 + \frac{4l-8x}{l^2} U_2 + \frac{4x-l}{l^2} \right. \\ & \cdot U_3 \left. \right] dx + \frac{EF}{2} \int_0^l \left[\frac{4x-3l}{l^2} U_3 + \frac{4l-8x}{l^2} U_4 \right. \\ & + \left. \frac{4x-l}{l^2} U_5 \right]^2 dx - \alpha EF \int_0^l \left[\frac{2x^2-3lx+l}{l^2} T_3 \right. \\ & + \frac{4l-4x^2}{l^2} T_4 + \left. \frac{2x^2-lx}{l^2} T_5 \right] \times \left[\frac{4x-3l}{l^2} U_3 \right. \\ & + \left. \frac{4l-8x}{l^2} U_4 + \frac{4x-l}{l^2} U_5 \right] dx + \frac{EF}{2} \\ & \cdot \int_0^l \left[\frac{4x-3l}{l^2} U_5 + \frac{4l-8x}{l^2} U_6 + \frac{4x-l}{l^2} U_7 \right]^2 dx \\ & - \alpha EF \int_0^l \left[\frac{2x^2-3lx+l}{l^2} T_5 + \frac{4l-4x^2}{l^2} T_6 \right. \\ & + \left. \frac{2x^2-lx}{l^2} T_7 \right] \times \left[\frac{4x-3l}{l^2} U_5 + \frac{4l-8x}{l^2} U_6 \right. \\ & + \left. \frac{4x-l}{l^2} U_7 \right] dx = \frac{EF}{6l_1} (7U_1^2 + 16U_2^2 + 7U_3^2 \\ & - 16U_1U_2 + 2U_1U_3 - 16U_2U_3) - \alpha EF \left(-\frac{1}{2} T_1 U_1 \right. \\ & + \frac{2}{3} T_1 U_2 - \frac{1}{6} T_1 U_3 - \frac{2}{3} T_2 U_1 + \frac{2}{3} T_2 U_3 + \frac{1}{6} T_3 U_1 - \frac{2}{3} \\ & \cdot T_3 U_2 \left. \right) + \frac{EF}{6l_2} (7U_3^2 + 16U_4^2 + 7U_5^2 - 16U_3U_4 \\ & + 2U_3U_5 - 16U_4U_5) - \alpha EF \left(\frac{2}{3} T_3 U_4 - \frac{1}{6} T_3 U_5 - \frac{2}{3} \right. \\ & \cdot T_4 U_3 + \frac{2}{3} T_4 U_5 + \frac{1}{6} T_5 U_3 - \frac{2}{3} T_5 U_4 \left. \right) + \frac{EF}{6l_3} (7U_5^2 \end{aligned}$$

$$\begin{aligned}
& + 16U_6^2 + 7U_7^2 - 16U_5U_6 + 2U_5U_7 - 16U_6U_7) \\
& - \alpha EF \left(\frac{2}{3}T_5U_6 - \frac{1}{6}T_5U_7 - \frac{2}{3}T_6U_5 + \frac{2}{3}T_6U_7 + \frac{1}{6} \right. \\
& \cdot T_7U_5 - \frac{2}{3}T_7U_6 + \frac{1}{2}T_7U_7) \\
\end{aligned} \tag{33}$$

Due to the pinch of both ends of the rod, $U_1 = U_7 = 0$.

By minimizing this functional on the nodal displacements U_2, U_3, \dots, U_6 , a resolving system of linear algebraic equations is constructed for the desired quantities, taking into account the simultaneous presence of heterogeneous heat sources and thermal insulation

$$\begin{aligned}
(1) \quad & \frac{\partial \Pi}{\partial U_2} = 0; \\
& \Rightarrow \frac{EF}{6l_1} (32U_2 - 16U_3) - \alpha EF \left(\frac{2}{3}T_1 - \frac{2}{3}T_3 \right) = 0; \\
(2) \quad & \frac{\partial \Pi}{\partial U_3} = 0; \\
& \Rightarrow EF \left[\left(\frac{14U_3 - 16U_2}{16l_1} \right) + \left(\frac{14U_3 - 16U_4 + 2U_5}{16l_2} \right) \right] - \alpha EF \left(-\frac{1}{6}T_1 + \frac{2}{3}T_2 - \frac{2}{3}T_4 + \frac{1}{6}T_5 \right) = 0; \\
(3) \quad & \frac{\partial \Pi}{\partial U_4} = 0; \\
& \Rightarrow \frac{EF}{6l_2} (32U_4 - 16U_3 - 16U_5) - \alpha EF \left(\frac{2}{3}T_3 - \frac{2}{3}T_5 \right) = 0; \\
(4) \quad & \frac{\partial \Pi}{\partial U_5} = 0; \\
& \Rightarrow EF \left[\left(\frac{14U_5 + 2U_3 - 16U_4}{16l_2} \right) + \left(\frac{14U_5 - 16U_6 + 2U_7}{16l_7} \right) \right] - \alpha EF \left(-\frac{1}{6}T_3 + \frac{2}{3}T_4 - \frac{2}{3}T_6 + \frac{1}{6}T_7 \right) = 0; \\
(5) \quad & \frac{\partial \Pi}{\partial U_6} = 0; \\
& \Rightarrow \frac{EF}{6l_3} (32U_6 - 16U_5 - 16U_7) - \alpha EF \left(\frac{2}{3}T_5 - \frac{2}{3}T_7 \right) = 0.
\end{aligned} \tag{34}$$

By solving the latter system, the values U_2, U_3, \dots, U_6 are determined. According to them, the displacement field is constructed within three discrete elements.

$$\begin{aligned}
U^{(I)}(x) &= \frac{4lx - 4x^2}{l^2} \cdot U_2 + \frac{2x^2 - lx}{l^2} \cdot U_3 \\
U^{(II)}(x) &= \frac{2x^2 - 3lx + l^2}{l^2} \cdot U_3 + \frac{4lx - 4x^2}{l^2} \cdot U_4 \\
&+ \frac{2x^2 - lx}{l^2} \cdot U_5 \\
U^{(III)}(x) &= \frac{2x^2 - 3lx + l^2}{l^2} \cdot U_5 + \frac{4lx - 4x^2}{l^2} \cdot U_6
\end{aligned} \tag{35}$$

4. Analysis of the Obtained Results

For the practical application of the above method and algorithm, we take the following initial data:

$$\begin{aligned}
L &= 3 \text{ cm}; \\
r &= 1 \text{ cm}; \\
\alpha &= 0,0000125 \text{ } 1/^\circ\text{K}; \\
E &= 2 \cdot 10^6 \text{ kG/cm}^2; \\
K_{xx} &= 100 \text{ watt/cm} \cdot ^\circ\text{K}; \\
h_1 = h_2 &= 10 \text{ watt/cm}^2 \cdot ^\circ\text{K}; \\
T_{axis1} = T_{axis2} &= 40^\circ\text{K}; \\
q &= -500 \text{ watt/cm}^2;
\end{aligned} \tag{36}$$

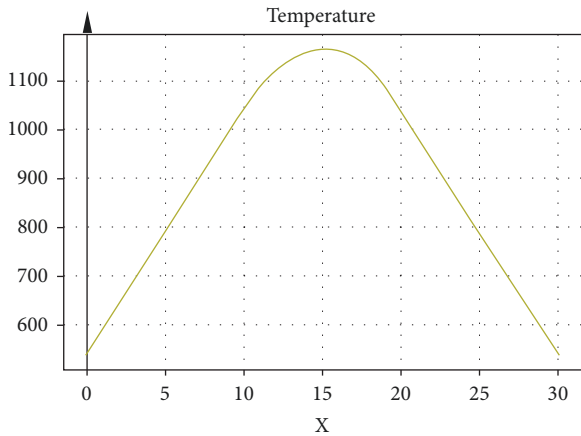


FIGURE 4: Temperature dependence T along the length of the rod.

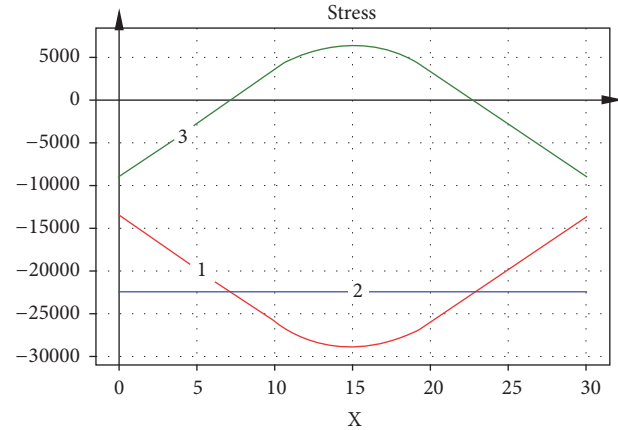


FIGURE 6: Stress Dependencies along the length of the rod. (1) Law distribution of temperature component of stresses $\sigma_T(x)$; (2) law distribution of thermoelastic component of stresses $\sigma(x)$; (3) law distribution of elastic component of stresses $\sigma_x(x)$.

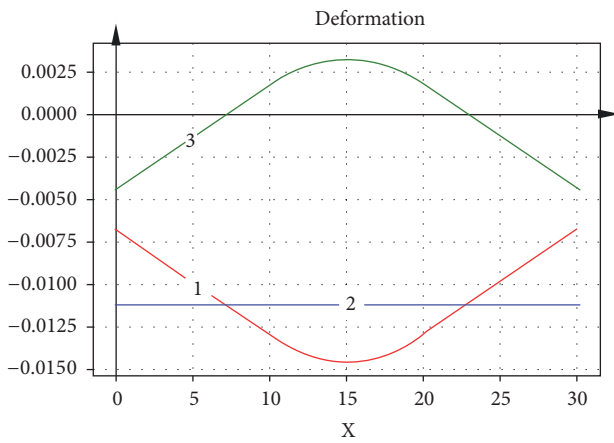


FIGURE 5: Dependencies deformations along the length of the rod. (1) Distribution law of temperature component of deformation $\epsilon_T(x)$; (2) law distribution of thermoelastic component of deformation $\epsilon(x)$; (3) law distribution of elastic component of deformation $\epsilon_x(x)$.

with these initial data, the resulting solution is shown in Figures 4–7.

For the numerical solution of the problem under consideration, the rod under study was discretized by $n = 24$ —discrete elements of the same length $l = L/n = 30/24 = 1,25\text{cm}$. The side surface of the first and last 8 elements is fully insulated. The heat flux $q = -500\text{watt}/\text{cm}^2$ is supplied to the lateral surface of the middle 8 elements.

From Figure 4, it is seen that, due to the symmetry of the problem under consideration, at the ends of the rod the temperature values will be $T(x = 0) = T(x = L) = 540^\circ\text{K}$. At that time, the highest temperature occurs in the middle of the rod, $T_x(x = L/2) = 1165^\circ\text{K}$. It can also be seen from Figure 4 that the temperature distribution field along the length of the rod under study has a parabolic character.

The laws of distribution of the three component deformations are shown in Figure 5. Here, the distribution field of the temperature component of deformation $\epsilon_T(x)$ has

a compressive character along the entire length of the rod under study. It has a parabolic shape with a bulge down. Its value at the ends of the investigated rod will be $\epsilon_T(x = 0) = \epsilon_T(x = L) = -0.0675$. At the time in the middle of the rod, it has $\epsilon_T(x = L/2) = -0.014562$. This shows that in the middle of the rod the temperature component of the deformation will be 2.157 times greater than that at the end of the rod. At that time, the value of the thermoelastic component of deformations $\epsilon(x)$ will be constant along the length of the rod and $\epsilon(x) = -0.0112$. The behavior of the elastic component of deformation will be of alternating sign. For example, in the middle part of the rod, where the heat flux is supplied, the elastic component of deformation $\epsilon(x)$ has a tensile character. Amplitude $\epsilon_x(x = L/2) = -0.033$. At that time, the first and last 1/3 of the rod will experience compressive $\epsilon_x(x)$. It should be noted that at the ends of the rod $\epsilon_x(x = 0) = \epsilon_x(x = L) = -0.0045$. In general, the distribution field $\epsilon_x(x)$ has a parabolic character, convex at the top. In the relevant generalized Hooke's law, the behavior of the stress components will be appropriate for the corresponding component strain (Figure 6).

The values of the thermoelastic component of stress $\sigma(x)$ along the entire length of the rod will be constant $\sigma(x) = -22528\text{kG}/\text{cm}^2$. However, the law of distribution of the temperature component of voltage $\sigma_T(x)$ will have a parabolic character, bulge down, and it will have a compressive character along the entire length of the rod. The values of $\sigma_T(x)$ at the ends of the rod will be $\sigma_T(x = 0) = \sigma_T(x = L) = -13500\text{kG}/\text{cm}^2$. At that time in the middle of the rod $\sigma_T(x = L/2) = -29125\text{kG}/\text{cm}^2$. This shows that in the middle of the bar the value of σ_T will be 2.157 times more than that at its ends. The elastic component of stress $\sigma_x(x)$ in the first and last 1/3 of the rod behaves as compressive, and in the middle 1/3 as tensile. With this

$$\begin{aligned} \sigma_x(x = 0) &= \sigma_x(x = L) = -9027\text{ kG}/\text{cm}^2, \\ \sigma_x\left(x = \frac{L}{2}\right) &= 6597\text{ kG}/\text{cm}^2. \end{aligned} \tag{37}$$

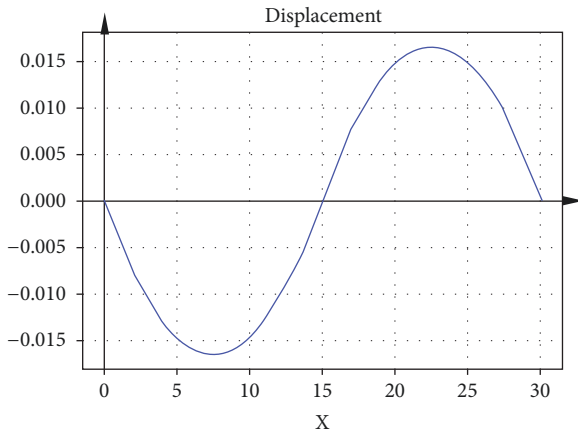


FIGURE 7: Dependence of displacement along the length of the rod.

The distribution law of the displacement of the rod sections is not shown in Figure 7. From this figure, it is clear that all sections of the left half of the rod are moved against the direction of the axis ox , and sections of the right half are shifted in the direction of the axis of the oh . This process is due to the presence on the surface of the middle 1/3 of the investigated rod summed heat flux. At that time, the amplitude of the displacement of the section whose coordinate $x = 7.5$ cm will be equal to $U(x=7.5) = -0.01627$ cm. Similarly, we have that $U(x=22.5) = 0.01627$ cm. This shows that the process under study is strictly symmetric about the middle of the rod.

5. Conclusion

The developed method based on the fundamental laws of energy conservation, a computational algorithm, and an application program in Python allows automating the construction of resolving systems of equations taking into account the natural boundary conditions for rods of limited length under the influence of dissimilar types of heat sources. The developed system also allows determining the laws of temperature distribution, all components of deformations and stresses, and displacements. In this regard, it can be stated that the developed method, algorithm, and Python programs are relatively universal in the sense of studying the steady thermo-stress-strain state of the supporting core elements of strategic equipment under the influence of various local heat sources. In this case, the obtained numerical results will differ in high accuracy, since these results satisfy the fundamental laws of energy conservation.

Data Availability

The data used to support the findings of this paper are available from the corresponding author upon request.

Conflicts of Interest

The authors declare that they have no conflicts of interest.

References

- [1] S. Timoshenko and J. N. Goodyear, *Theory of Elasticity*, McGRAW-Hill. Book. Company. Inc., 1987.
- [2] K. S. Shibib, M. A. Minshid, and N. E. Alattar, "Thermal and stress analysis in Nd:YAG laser rod with different double end pumping methods," *Thermal Science*, vol. 15, suppl. 2, pp. S399–S407, 2011.
- [3] K. S. Shibib, M. M. Tahir, and H. I. Qatta, "Analytical model of transient temperature and thermal stress in continuous wave double-end-pumped laser rod: thermal stress minimization study," *Pramana—Journal of Physics*, vol. 79, no. 2, pp. 287–297, 2012.
- [4] D. L. Logan, *A First Course in the Finite Element Method*, CENGAGE Learning, 2012.
- [5] Y. Orçan, "Thermal stresses in a heat generating elastic-plastic cylinder with free ends," *International Journal of Engineering Science*, vol. 32, no. 6, pp. 883–898, 1994.
- [6] V. I. Andreev and R. A. Turusov, "Nonlinear modeling of the kinetics of thermal stresses in polymer rods," in *Advanced Materials and Structural Engineering*, Hu, Ed., Taylor & Francis Group, London, UK, 2016.
- [7] Y. I. Nyashin, V. Y. Kiryukhin, and F. Ziegler, "Control of thermal stress and strain," *Journal of Thermal Stresses*, vol. 23, no. 4, pp. 309–326, 2000.
- [8] K. K. Gornostaev, A. V. Kovalev, and Y. V. Malygina, "Stress-strain state in an elastoplastic pipe taking into account the temperature and compressibility of the material," *Journal of Physics: Conference Series*, vol. 973, 2018.
- [9] B. F. Shorr, "Thermal integrity in mechanics and engineering," in *Foundations of Thermoelasticity*, pp. 33–55, Springer, Berlin, Germany, 2015.
- [10] O. C. Zienkiewicz and K. Morgan, *Finite Elements & Approximation*, John Wiley & Sons, Inc., New York, NY, USA, 1983.
- [11] O. C. Zienkiewicz and R. L. Taylor, *The Finite Element Method*, Butterworth-Heinemann, Oxford, UK, 5th edition, 2000.

